

Synthesis of Polycardanol Using $\text{BF}_3 \cdot \text{O}(\text{C}_2\text{H}_5)_2$ as Initiator: Influence of Polymerization Conditions on Reaction Products

Maximiliano F. Martins,^a Thiago M. Aversa,^b Carla Michele F. da Silva,^{id c}
Edilson D. da Silva^c and Elizabete F. Lucas^{id *,a,c}

^aPrograma de Engenharia Metalúrgica e de Materiais,
Instituto Alberto Luiz Coimbra de Pós-Graduação e Pesquisa de Engenharia,
Universidade Federal do Rio de Janeiro, (PEMM/COPPE/UFRJ), Av. Horácio de Macedo, 2030,
Bloco F, Cidade Universitária, 21941-598 Rio de Janeiro-RJ, Brazil

^bInstituto Federal de Educação, Ciência e Tecnologia do Rio de Janeiro (IFRJ),
Av. República do Paraguai, 120, Vila Sarapu, 25050-100 Duque de Caxias-RJ, Brazil

^cInstituto de Macromoléculas, Universidade Federal do Rio de Janeiro, (IMA/UFRJ),
Av. Horário de Macedo, 2030, Bloco J, Cidade Universitária, 21941-598 Rio de Janeiro-RJ, Brazil

Cardanol acts to stabilize asphaltene particles in crude oil, but its derivative polycardanol, synthesized with $\text{BF}_3 \cdot \text{O}(\text{C}_2\text{H}_5)_2$ as initiator, exhibits divergent behavior, acting as both asphaltene stabilizer and flocculant. This behavior could be related to structural differences in polycardanol samples. Therefore, in this work, we study the influence of some polymerization conditions (monomer purity, initiator concentration, and reaction time) on the structures and molar masses of the reaction products, and the reaction conversion. The materials were characterized by size-exclusion chromatography and hydrogen and carbon nuclear magnetic resonance. When reacting with distilled cardanol, the conversion, the molar mass, and the homogeneity of structures increased as increasing initiator concentration in the range tested (1-3% m/m). For both monomers (different purity degrees), when using a lower initiator concentration (1% m/m), the product contained a larger amount of unreacted monomer and different structures were obtained due to the occurrence of rearrangements. The presence of triolefinic molecules in the monomer provoked crosslinked structures for higher initiator concentration (2-3% m/m). This study elucidated the differences among the reaction products of polycardanol.

Keywords: cardanol, polycardanol, boron trifluoride, Friedel-Crafts, polymerization

Introduction

The growing concern over environmental preservation has intensified the search for renewable natural resources with the potential for applications in different industrial processes.¹⁻³ In this context, cardanol, an abundant and inexpensive natural compound, has been investigated as an alternative to petrochemicals for certain applications.^{4,5}

Cardanol is a phenolic compound containing a *meta*-substituted aliphatic chain of fifteen carbons in its structure, with different degrees of saturation.^{6,7} The material is obtained as a byproduct of processing fruits/nuts from the cashew tree, a species cultivated in many

countries.^{6,8} The shells of the nuts of the cashew tree contain a viscous oil with dark brown color that is caustic and inflammable, called cashew nut shell liquid (CNSL). Besides cardanol, this oil contains three other main compounds, anacardic acid, cardol, and 2-methyl cardol, along with lesser occurrences of polymers.⁸ CNSL can be obtained by several different processes and depending on the method employed, variations in the composition of the material have been reported.⁹ Extractions performed in the absence of heat give rise to natural CNSL with high content of anacardic acid, obtained by cold pressing or via extraction with solvents such as benzene or toluene. On the other hand, thermal-mechanical treatment of the nuts at temperatures near 180 °C causes the almost complete conversion of anacardic acid into cardanol through the decarboxylation reaction. As a result, the material obtained

*e-mail: elucas@ima.ufrj.br

Editor handled this article: Brenno A. D. Neto (Associate)

has low acid levels and is called technical CNSL. Besides this, heating unleashes polymerization reactions of the unsaturated compounds, causing the aging of the oil.^{8,10,11}

Cardanol can be obtained with high conversion rates from technical CNSL by distilling the oil in a low-pressure system. At the end of the process, an opaque to translucent yellowish liquid is separated out, containing saturated (ca. 5%), mono-olefinic (ca. 49%), diolefinic (ca. 17%) and triolefinic (ca. 29%) cardanol, besides traces of other compounds present in CNSL.⁴ The liquid obtained tends to darken with storage due to the aging provoked by the polymerization reaction among the species present in its composition.^{12,13} A second distillation of the liquid separates cardanol from the other compounds contained in the oil (cardol, 2-methyl cardol and polymeric materials), yielding a product with greater purity.^{8,14}

The structure of cardanol has chemical and physicochemical characteristics that differentiate it from similar compounds, mainly the existence of several reaction sites. The hydroxyl group of the phenol, the aromatic ring and the unsaturations of the aliphatic chain enable obtaining various types of functionalization of the cardanol molecules, making it a valuable starting material for the synthesis of various compounds, including polymers.^{8,15-17} The literature describes the polymerization of cardanol through different methods. Polycondensation of the material is achieved by the reaction of the phenol group with aldehydes, obtaining as a product novolac resins.¹⁸⁻²⁰ On the other hand, polymerization using Lewis acids as cationic initiators can occur either by substitution on the aromatic ring of cardanol, through a Friedel-Crafts aromatic alkylation mechanism, or by the occurrence of etherification involving the phenol OH group during synthesis. However, no differences in the produced structures were identified.²¹

Due to the structural similarity of cardanol with substances such as dodecylbenzene sulfonic acid, 4-*n*-nonylphenol and 4-*n*-dodecylphenol, all of which are chemical inhibitors used in crude oil with great potential for precipitation of asphaltenes,²²⁻²⁶ therefore studies have been conducted to evaluate its ability to stabilize asphaltenes.²⁷

Asphaltenes are a class of substances present in crude oil characterized as the heaviest and most polar fraction. Their structures are composed of condensed polyaromatic nuclei associated with cyclical and aliphatic side chains containing representative contents of heteroatoms in their structure, such as oxygen, nitrogen and sulfur, along with traces of some metals. Due to these characteristics, the structures of asphaltenes are highly complex and variable, making them difficult to identify.²⁸⁻³² The high molar mass, structural heterogeneity and the presence of functional groups enable their destabilization in response to variations

of pressure, temperature and composition of the petroleum in production conditions.^{33,34} One of the theories accepted regarding the mechanism of stabilizing asphaltenes involves the presence of surfactant molecules, whose polar groups interact with the asphaltenes and whose nonpolar groups interact with the other components of the oil. The resins contained in the petroleum exercise this role.^{28,30,35-38}

The inclusion of polycardanol in studies of the stabilization of asphaltenes began due to the good performance of cardanol in relation to inhibitors with recognized action, prompting their incorporation in this field of research.³⁹ However, although in most cases polymers have better properties than the monomers from which they originate, some authors disagree about the activity of polycardanol, obtained using boron trifluoride diethyl etherate ($\text{BF}_3 \cdot \text{O}(\text{C}_2\text{H}_5)_2$) as initiator, as an additive to modify the asphaltenes phase behavior. The results revealed that different polycardanol samples presented dissimilar performances, acting as asphaltenes stabilizer or flocculant.^{39,40} Despite the importance of the structure-property relationship, no studies were found on the exact composition of the products of polymerizing cardanol, considering not only the structure of the resulting polymer but also the distribution of molar mass and content of unreacted material in its composition. These parameters can have a significant influence on the product of the reaction, not only for the stabilization/flocculation of asphaltenes, but also for other applications.

Thus, this work presents an in-depth study of the polymerization reaction of cardanol using $\text{BF}_3 \cdot \text{O}(\text{C}_2\text{H}_5)_2$ as initiator, to shed light on the influence of the cardanol purity, the monomer:initiator ratio and reaction time on the conversion rate of the reaction, the molar mass and dispersity of the polymer, as well as the intermediate and final structures of the polymerization reaction. For this purpose, we synthesized six substances and characterized them by size-exclusion chromatography (SEC) and nuclear magnetic resonance (^1H and ^{13}C NMR).

Experimental

Materials

Technical cardanol, used as monomer, was supplied by Satya Cashew Chemicals Pvt. Ltd. (Chennai, India). $\text{BF}_3 \cdot \text{O}(\text{C}_2\text{H}_5)_2$, with 99.0% purity, was used as initiator in the polymerization reactions, supplied by Sigma-Aldrich (São Paulo, Brazil). Deuterated chloroform (CDCl_3) with 99.8% purity, manufactured by Cambridge Isotopic Laboratory, was also supplied by Sigma-Aldrich (São Paulo, Brazil). Stabilized high-performance liquid chromatography

(HPLC) spectroscopy grade tetrahydrofuran (THF) with 99.8% purity was supplied by Tedia (Rio de Janeiro, Brazil). And commercial-grade toluene was supplied by Vetec Química Fina (Rio de Janeiro, Brazil).

Cardanol distillation

Cardanol previously stored in the laboratory, designated in this work aged cardanol (ACN), was purified through the reduced pressure distillation technique, carried out at 25 mmHg and temperature varying between 265 and 275 °C. The purified material was called distilled cardanol (DCN).

Materials synthesis

All materials were obtained by bulk polymerization, using $\text{BF}_3 \cdot \text{O}(\text{C}_2\text{H}_5)_2$ as initiator. Reactions were conducted as described below. The monomer and initiator were homogenized for 5 min in a beaker with magnetic stirring. Then, the mixture was transferred to a Schlenk flask placed in an oil bath previously heated to 138 °C, and the system was kept under magnetic stirring during the reaction time. After the reaction time, the products were not purified. Table 1 shows the parameters defined for all syntheses performed in this work, as well as describes the codes assigned to each substance obtained. The PDCN2-3 showed high viscosity, requiring the use of toluene to remove it from the flask at the end of the reaction, which was subsequently evaporated.

Characterization

The number average molar weight (\bar{M}_n), weight average molar weight (\bar{M}_w) and dispersity (\bar{D}) of the materials were obtained using size-exclusion chromatography (SEC). The analyses were carried out with a Malvern Panalytical chromatograph Viscotek GPC Max VE2001 (Texas, United States), equipped with Shodex chromatographic columns (model KF-G 4A pre-column and column models

KF-804L and KF-805L) and a refractive index detector. The equipment was calibrated from a universal calibration curve using a polystyrene monodisperse standard. The concentration of the samples was 3 mg mL⁻¹ and THF was used as solvent and eluent.

The structural characterization of the materials was performed by ¹H and ¹³C NMR spectroscopy using a Bruker Avance III 500 MHz spectrometer (Massachusetts, United States). The sample concentration was 45 mg mL⁻¹ in CDCl₃ and tetramethylsilane (TMS) was used as internal standard. The chemical shifts of the sample signals were expressed in parts *per* million (ppm) relative to the TMS signal. All NMR spectra were obtained with acquisition time (d1) of 1.0 s for ¹H and 2.0 s for ¹³C; pulse delay (p1) of 10.700 μs for ¹H and 10.750 μs for ¹³C; and spectral width (SWH) of 10.00 kHz for ¹H and 29.76 kHz for ¹³C. The ¹³C nuclei were observed uncoupled from the protons (¹³C{¹H}). Chemical displacement estimates of carbon nuclei for the structures proposed in this work were obtained using the PerkinElmer ChemDraw® Professional v.18.2.0.48 software.⁴¹ In order to validate the hypotheses established from the predictions made, distortionless enhancement by polarization transfer (DEPT-135) NMR analyses were performed with two samples that exhibited divergence of signals in the spectra. In addition, a 2D DEPT-HSQC (heteronuclear single quantum coherence) NMR analysis was performed for one of these samples, to confirm the new hypotheses after the interpretation of the DEPT experiment.

Results and Discussion

Materials synthesis

Initially, we established as the parameters for synthesis the reaction times of 2 and 4 h and initiator concentrations of 1, 2, and 3% (m/m). However, the reaction of ACN with initiator concentrations greater than 1% led to the formation of crosslinked products, so 1% was the only initiator percentage used. To better understand the phenomenon and in an attempt to identify the agent responsible for

Table 1. Synthesis parameters in the polymerization reaction of cardanol using $\text{BF}_3 \cdot \text{O}(\text{C}_2\text{H}_5)_2$

Cardanol sample	Cardanol sample code	Reaction time / h	Initiator concentration / (m/m %)	Material code
Aged cardanol	ACN	2	1	PACN2-1
		4	1	PACN4-1
Distilled cardanol	DCN	2	1	PDCN2-1
			2	PDCN2-2
		4	3	PDCN2-3
			3	PDCN4-3

the crosslinking, we purified the ACN by distillation to obtain the DCN. This process made it possible to perform the reactions at the three initiator concentrations initially established (1, 2 and 3% by mass). Therefore, six materials were synthesized from the cardanol samples (ACN and DCN), as shown in Table 1.

After the distillation process, the liquid obtained was translucent with yellowish color, in contrast to the original appearance of the ACN (dark purple and opaque), indicating alteration of the composition of the distilled material. The appearance of the two materials is in accordance with the descriptions in the literature.¹²

SEC analysis

The analyses of molar mass and molar mass distribution of the materials are presented in Figure 1, with the indication of the values of \bar{M}_n , \bar{M}_w , and \mathcal{D} of each sample.

The chromatogram of the reagent ACN had relatively narrow \mathcal{D} but indicated the presence of species with higher molar mass in the composition than that of pure cardanol

(ca. 301 g mol⁻¹). This behavior was expected, due to the previous reactions observed during the natural aging process of the material.¹² Likewise, the chromatogram of the DCN also presented a relatively narrow \mathcal{D} , but broader than the distribution curve of the ACN, producing materials with higher values of \bar{M}_n and \bar{M}_w . The greater occurrence of species with higher molar mass in the composition of the DCN was probably related to the heating to which it was submitted during distillation, with the higher temperature being responsible for triggering reactions among the species present in the material.¹⁰

The molar mass distribution curves of all the synthesized samples using 1-2% initiator (PACN2-1, PACN4-1, PDCN2-1, and PDCN2-2) indicated the presence of a significant quantity of unreacted cardanol. Despite the low conversion, the materials PACN2-1, PACN4-1 and PDCN2-2 had values of \bar{M}_w (6,396, 12,676 and 3,282 g mol⁻¹, respectively) that indicated the formation of a polymer, contrary to what we observed for the PDCN2-1 ($\bar{M}_w = 1,769$ g mol⁻¹), which was limited to the formation of oligomers. On the other hand, PDCN2-3 and PDCN4-3

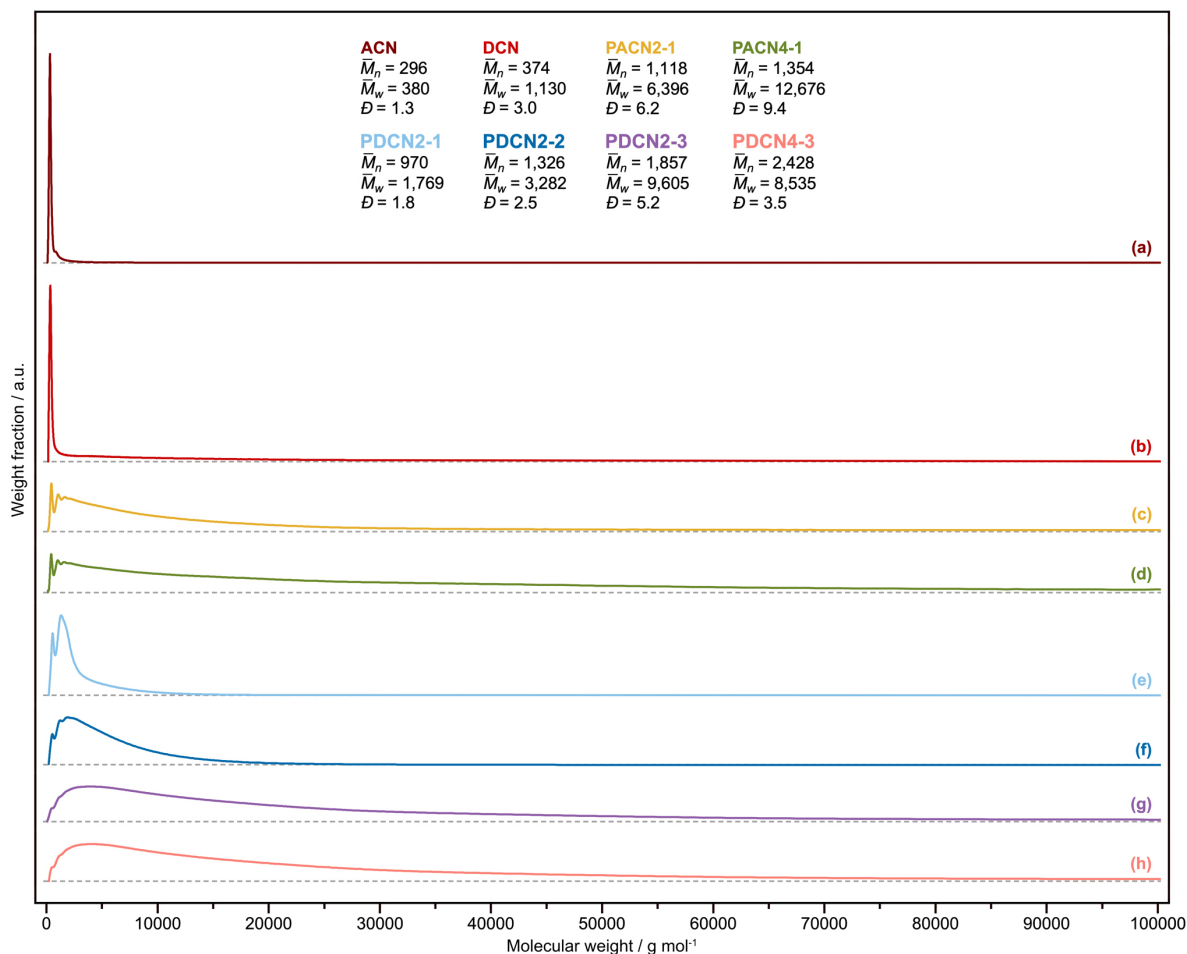


Figure 1. SEC chromatograms of the synthesized materials, containing the mean values of molar mass and \mathcal{D} of all samples. (a) ACN; (b) DCN; (c) PACN2-1; (d) PACN4-1; (e) PDCN2-1; (f) PDCN2-2; (g) PDCN2-3; (h) PDCN4-3.

chromatograms indicated high conversion of the reagent, but there was still a small shoulder in the region of low molar mass, attributed to a small quantity of unreacted cardanol. This can probably be attributed to the presence of material with a saturated structure, unable to react with the initiator during synthesis. Because of the higher conversion, the products PDCN2-3 and PDCN4-3 presented a broader \bar{M}_w than the PDCN2-1 and PDCN2-2, obtained with the same reagent (DCN).

Analysis of the influence of the initiator concentration on the synthesis of the products obtained from the DCN revealed that the molar mass increased with the rising quantity of initiator, as reported in the literature.⁴² In contrast, the variation of the reaction time had a different influence on the synthesis carried out with each reagent. For the two products obtained from the reagent ACN, the longest reaction time (4 h) produced higher values of \bar{M}_w and \bar{M}_n of the PACN4-1 in comparison with the PACN2-1. The opposite occurred between the PDCN2-3 and PDCN4-3, where the latter material (obtained with a reaction time of 4 h) had narrower \bar{M}_w than the former. That behavior suggests that the reactions did not occur in the same way for each type of material. Besides this, the chromatograms of the materials obtained from each reagent revealed another important characteristic: among all the materials synthesized, the products obtained from the ACN had higher values of \bar{M}_w and \bar{M}_n , and these values were also

larger than those of the PDCN2-3 and PDCN4-3, in which we employed a higher initiator concentration for synthesis (3%). These results are probably related to the difference in the composition of the reagents. It is important to stress that only after the purification of the ACN it was possible to inhibit the crosslinking process during the synthesis, demonstrating the existence of a fundamental difference between the two reagents.

^1H NMR spectra of ACN and DCN

Figure 2 presents the ^1H NMR spectra of the reagents ACN and DCN, with attribution of the signals observed to the corresponding positions of each hydrogen in the structures of cardanol and cardol.

In the region of the aromatic hydrogens, between 7.15 and 6.00 ppm, the signals were at a (t, δ 7.06 ppm), b (d, δ 6.67 ppm), c (s, δ 6.58 ppm) and d (d, δ 6.56 ppm), referring to the benzene protons, which determine the *meta*-disubstitution pattern of the aromatic ring of cardanol, with these signals being present in both spectra.^{43,44} This region also contained the signals at e (s, δ 6.15) and f (s, δ 6.10 ppm), attributed to the aromatic hydrogens of cardol.⁴⁵ Both signals were present in the ACN spectrum, but in the DCN spectrum, only the signal at e occurred with lower intensity than in the ACN spectrum, indicating a reduction in the concentration of cardol in the composition

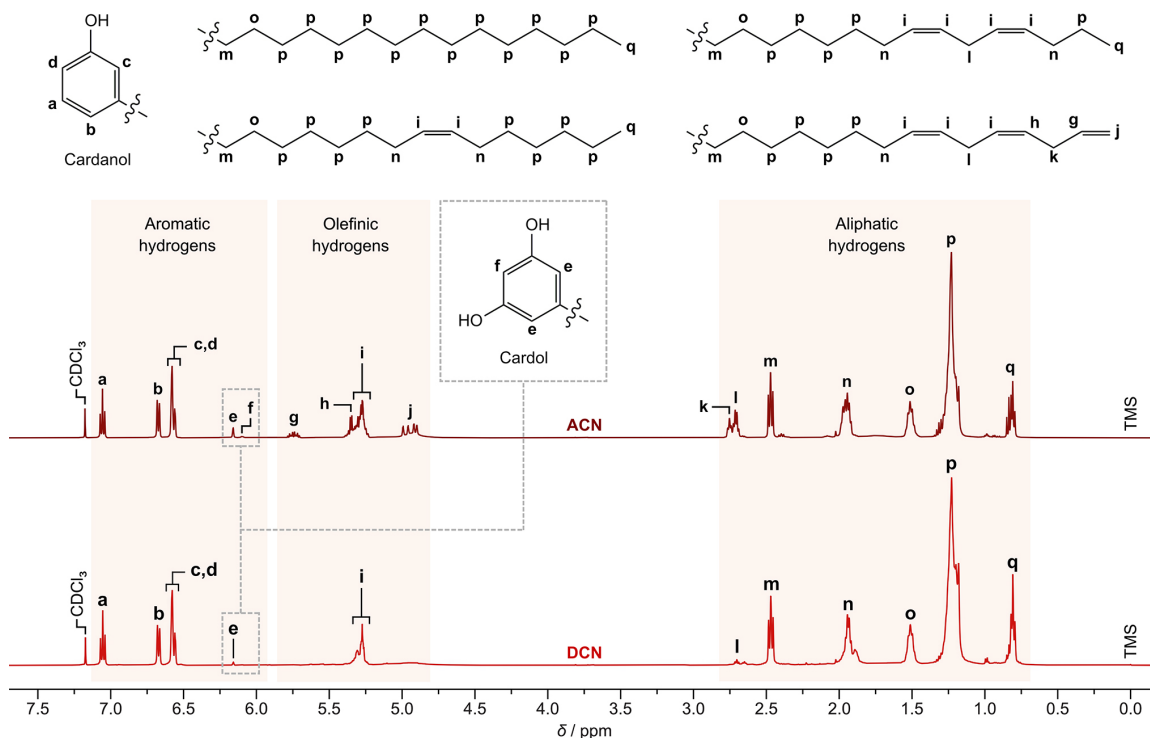


Figure 2. Comparison between the ^1H NMR spectra (500 MHz, CDCl_3) of ACN and DCN and signal assignment to each hydrogen in the four structures of cardanol and cardol.

of the distilled material. This result was expected since elsewhere it has been reported that with each new distillation of cardanol, the product has higher purity.⁸ Due to the low concentration of cardol in both reagents, for practical purposes we disregarded its structure during the structural characterization of the products obtained.

The region of the olefinic hydrogens (between 5.85 and 4.80 ppm) indicated the main differences between the spectra analyzed. The signals at g (m, δ 5.74 ppm) and j (dd, δ 4.97 and 4.90 ppm), referring to the vinyl group in the triolefinic structure of cardanol, were observed only in the ACN spectrum. The absence of these signals in the DCN spectrum revealed that this structure was not present in the material purified by distillation. As a consequence, the signal at h (overlapping signals, δ 5.35 ppm), referring to one of the protons of the adjacent unsaturations of the vinyl group in the triolefinic structure, also was absent in the DCN spectrum. Next, the overlapping signals at i (m, δ between 5.31 and 5.26 ppm) corresponded to the unsaturation protons inside each chain in the mono, di and triolefinic structures.⁴³ The pattern of signals at i observed in the DCN spectrum (unfolding into two signals) suggested the presence of a diolefinic structure of the purified material.

The region between 2.80 and 0.70 ppm contained signals related to the aliphatic protons of cardanol.^{44,46} The signals at k and l (t, δ 2.71 and 2.70 ppm) refer to the protons linked to the carbons positioned between the two olefinic groups in the hydrocarbon chain, where the signal at k is attributed to the allylic proton located between an unsaturation and the vinyl group in the triolefinic structure and the signal at l is attributed to the allylic protons between two unsaturations in the di and triolefinic structures. The signal at k was only present in the ACN spectrum, a result providing further confirmation that the triolefinic structure was not present in the distilled material. In turn, the presence of a signal at l in the DCN spectrum, albeit with low intensity, confirmed the hypothesis of the presence of a diolefinic structure in its composition, as suggested by the pattern of the signals at i, as described previously. The signals at m (t, δ 2.47 ppm), n (m, δ 1.95 ppm), o (p, δ 1.51 ppm), and p (m, δ 1.23 ppm) refer to the protons of methylene groups (CH₂) of the aliphatic chain. Finally, the signal at q (m, δ 0.82 ppm) refers to the terminal methyl group (CH₃) of the aliphatic chain in the saturated, mono-olefinic and diolefinic structures. This signal was more intense in the DCN spectrum than the ACN spectrum, indicating the higher concentration of these three structures in the distilled reagent. This behavior can be attributed to the separation of the triolefinic structure of the purified material, which remained in the flask together with the material that was not distilled. Besides this, there were

signals with low intensity at δ 2.40 and 1.00 ppm, which in the case of ACN can be related to reactions that occur spontaneously during the period the material is stored, while in the case of DCN, the reactions can be attributed to the heating of the material during distillation.^{10,12}

¹H NMR spectra of the synthesized materials

Reactions involving olefinic groups

Figure 3 presents the ¹H NMR spectra of the six products synthesized in this study. Once again, there were variations in the signals observed in the spectral region referring to the olefinic groups, indicating the existence of different final compositions of the products.

The spectra of the PACN2-1, PACN4-1, PDCN2-1, and PDCN2-2 contained signals related to the unsaturations of the side chain of cardanol. The presence of these signals is coherent with the low conversion of the reagent observed in the SEC analyses of these four products, indicated by the presence of the peak referring to unreacted cardanol in their chromatograms. Among these four materials, only the spectrum of PDCN2-2 did not exhibit signals referring to the vinyl group (m, δ 5.74 ppm, dd, δ 4.97 and 4.90 ppm) arising from the triolefinic structure. The presence of these signals in the spectra of the PACN2-1 and PACN4-1 was not surprising, because the triolefinic structure is present in the reagent ACN and there was incomplete conversion of these materials. On the other hand, the occurrence of signals referring to the vinyl group in the spectrum of the PDCN2-1 revealed that during the reactions involving the reagent DCN, the vinyl group was incorporated in the structure of the product, producing species that initially were not part of the composition of this reagent. Besides this, the pattern of signals observed in the spectrum of the PDCN2-1 was similar to the spectrum of the reagent ACN (Figure 2), indicating not only that the vinyl group was incorporated in the compound, but that the triolefinic structure of cardanol was also produced during the synthesis of this material. This behavior indicated the occurrence of parallel reactions to the polymerization reaction during the synthesis. A more detailed analysis of this phenomenon is presented in the "Rearrangement Reactions" sub-section. Besides this, the spectra of these four materials contained a signal at δ 1.89 ppm. Because it was not present in the spectra of the materials with high conversion (PDCN2-3 and PDCN4-3), the occurrence of this signal suggests the existence of different structures of the products formed in each group of materials.

Finally, the spectra of the materials PDCN2-3 and PDCN4-3 did not contain signals in the region corresponding to the olefinic groups, with consequent disappearance of the signal at δ 1.95 ppm referring

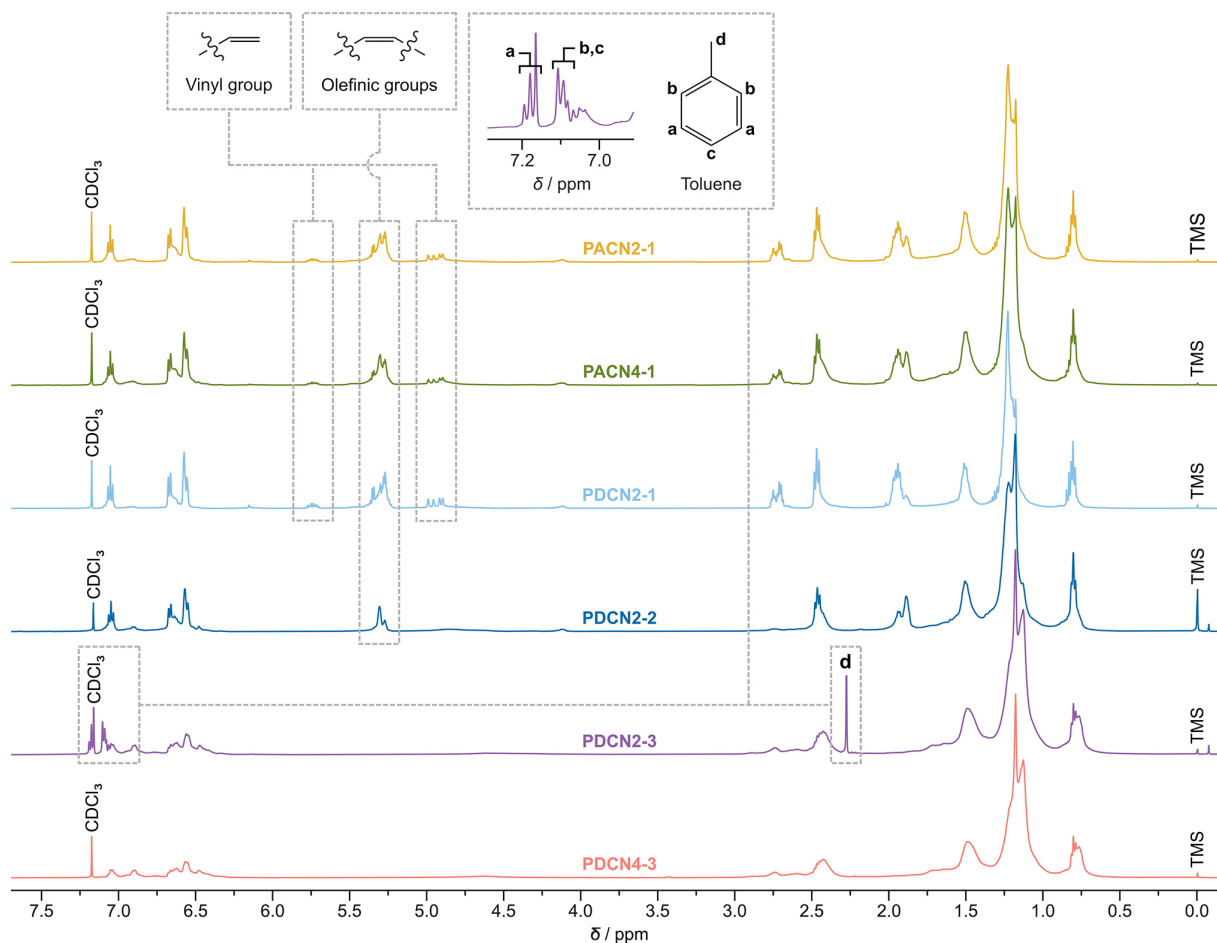


Figure 3. ^1H NMR spectra (500 MHz, CDCl_3) of the materials obtained from ACN and DCN.

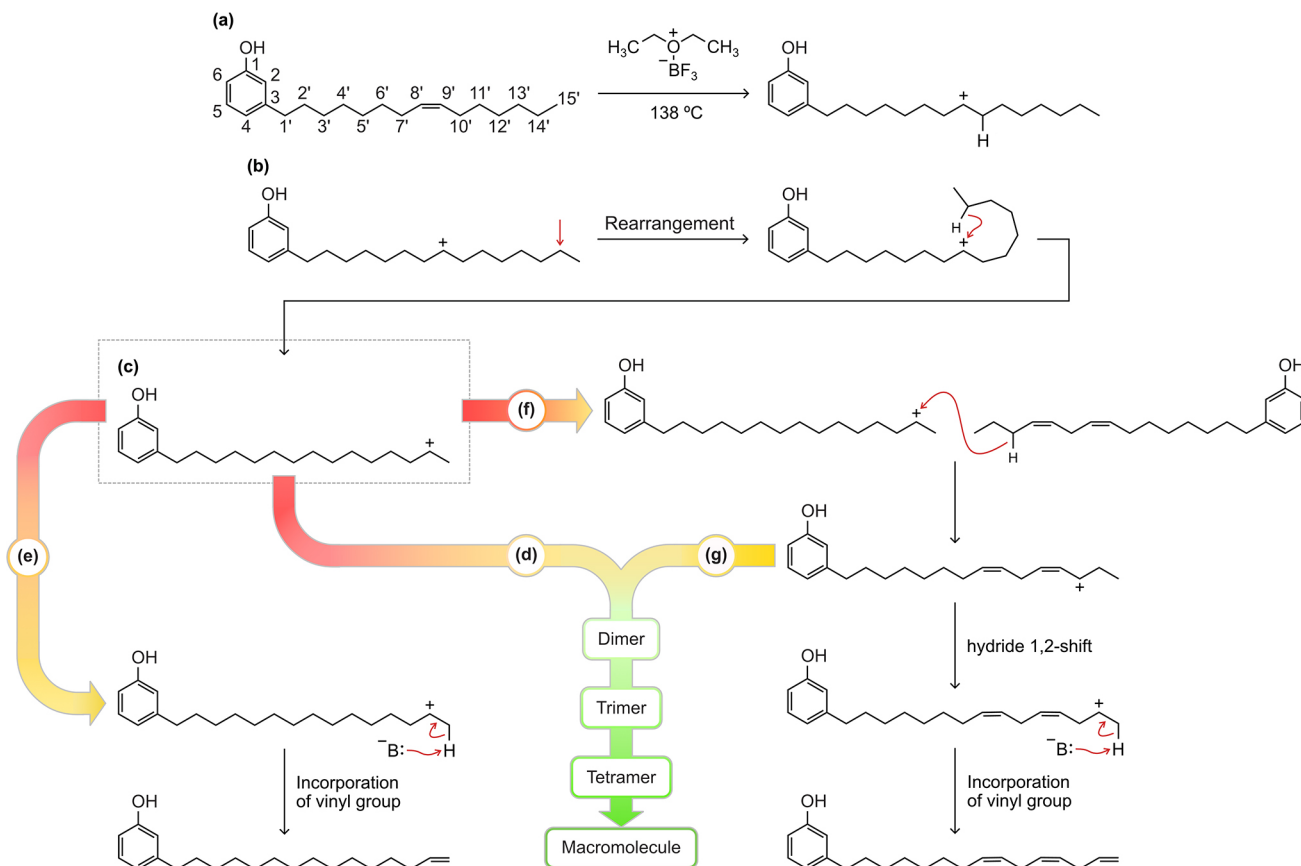
to the allylic protons adjacent to the double bonds in the hydrocarbon chain. The absence of these signals indicated that the unsaturations were totally converted during the synthesis of these materials, confirming that the shoulder referring to the unreacted cardanol present in the chromatograms of both materials indeed refers to the saturated structure of cardanol. Another important aspect observed in the spectra of these materials was the broadening of the signals resulting from the polymerization process of these compounds. Another peculiarity, this time only observed in the spectrum of PDCN2-3, was the appearance of signals referring to the solvent (toluene) used to remove the material from the flask at the end of the reaction. Figure 3 shows an expanded image of the spectral region between 7.30 and 6.90 ppm, indicating the signals of the benzene protons of the toluene (t, δ 7.18 ppm and overlapping signals, δ 7.10–7.08 ppm). The signal referring to the protons of the CH_3 group was present in a higher field in the spectrum, as a singlet of δ 2.25 ppm.⁴⁷

Rearrangement reactions

Considering the species present in the reagent DCN, the

intra and intermolecular reactions that occurred during the intermediate steps of the synthesis process can explain the incorporation of the vinyl group and consequent formation of the triolefinic structure in the product PDCN2-1. Scheme 1 describes the proposed reaction schemes, where obtaining the structures containing the vinyl group took place due to the rearrangement of the structure of the mono-olefinic cardanol.

Among the schemes proposed after reaction with a cationic initiator, a carbocation is formed by opening the double bond in the side chain of cardanol, enabling the incorporation of a proton in its structure (Scheme 1a). In the next step, the active center generated migrates to a position in the chain through the transfer of a hydride ion (Scheme 1b). The free rotation of the aliphatic chain then enables the repositioning of the positive charge to a more external position in the ring, on one of the carbons located at the end of the hydrocarbon chain. In this case, the most probable position is that of carbon 14' instead of carbon 15' (indicated by the arrow in Scheme 1b), due to the possibility of forming a more stable secondary carbocation. Based on the intermediary formed (Scheme 1c), three



Scheme 1. Reaction schemes to obtain structures of cardanol containing a vinyl group from a mono-olefinic cardanol.

routes are possible. In the first (Scheme 1d), the continued propagation of the chain occurs with the possible formation of an oligomer/polymer. In the second route (Scheme 1e), a Lewis base present in the reaction medium removes the proton located at the tip of the aliphatic chain of the molecule (carbon 15') and the pair of electrons then form the double bond of the vinyl group in the molecule structure. That reaction, although describing a possible route for incorporation of the vinyl group in the structure of cardanol, does not clarify the formation of the triolefinic structure in the reaction product.

The occurrence of the triolefinic structure can only be explained by a reaction between two species in the reaction medium, namely a carbocation and a diolefinic structure of the cardanol. Although this reaction can occur starting from any carbocation present in the reaction medium, it is reasonable to imagine that it involves the intermediate substance formed by the rearrangement of the chain (Scheme 1c), due to the positioning of the positive charge at the end of the chain, facilitating the approximation between the molecules involved in the reaction, leading us to the last route possible via the proposed intermediate substance (Scheme 1f). In this reaction, the carbocation, instead of having the vinyl group established by the attack

of the Lewis base (Scheme 1e), receives the transfer of the hydride ion of the diolefinic structure, which is probably the allylic hydrogen located at the 13' position of the carbon in the molecule (again due to the stability of the formed carbocation), generating a cardanol structure with a saturated hydrocarbon chain and a new intermediate substance with a diolefinic structure containing the carbocation. From the new intermediate substance, two new routes would be possible. The first one would occur in an analogous way to the reaction scheme proposed previously (Scheme 1d). The charge of the carbocation generated in the diolefinic structure would continue to propagate, generating dimers, trimers, tetramers, etc. (Scheme 1g). In the second route, the charge of the carbocation would migrate to the 14' carbon from the 1,2-shift of a hydride ion located on this carbon.⁴⁸ Once again, a Lewis base removes the proton located at the tip of the chain (carbon 15'), incorporating the vinyl group, resulting in the formation of a triolefinic structure of the cardanol.

It is important to stress that the spectra of all the materials synthesized with the reagent DCN did not indicate the presence of a triolefinic structure in the final composition, but this structure can be produced in an intermediate substance during the synthesis, with its

exhaustion in the reaction medium being promoted by the use of higher initiator concentrations or even by employing longer reaction time in some cases.

Reactions involving the aromatic ring and the OH group

In the region between 7.30 and 6.30 ppm, related to the aromatic hydrogens, it was possible to identify from the expanded spectra presented in Figure 4 the presence of signals related to the alteration of the structure of the aromatic ring in all the synthesized materials, with an increase in the intensity of these signals in proportion to the percentage of initiator used and the reaction time employed in each synthesis. In all the spectra, we observed an isolated doublet at δ 6.90 ppm, a second signal overlapping the original signals of cardanol at around δ 6.62 ppm, and finally an isolated singlet at δ 6.49 ppm.

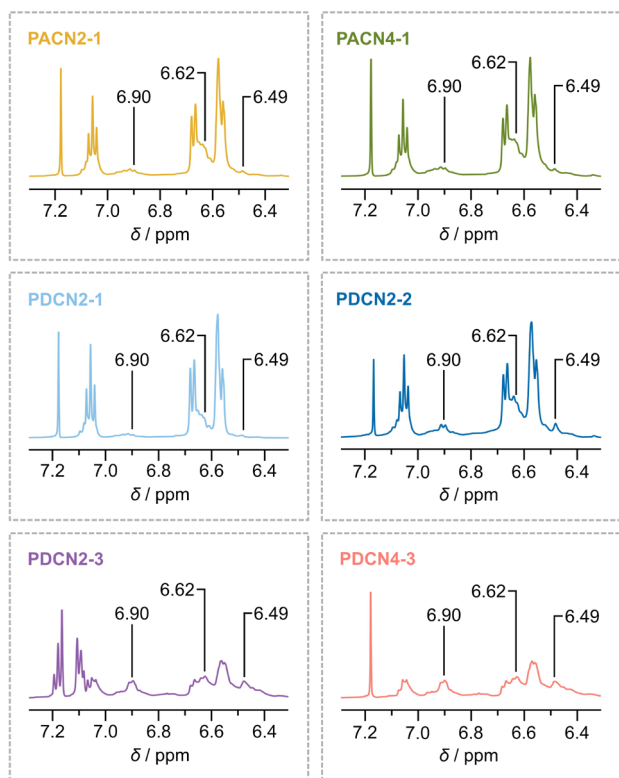


Figure 4. ^1H NMR spectra (500 MHz, CDCl_3) of the synthesized materials in the region between 7.30 and 6.30 ppm.

The reactivity of an aromatic ring is substantially affected by the presence of groups linked directly to its structure. For example, the main characteristic of an electron donor group is the availability of electrons to donate to the ring, hence making it more reactive. Another important aspect is that the orientation of entry of new substituent groups is also influenced by the characteristics of the group present in the ring. In the specific case of

cardanol, its aromatic ring has two groups in its structure, the OH group, a strong electron donor, and the alkyl group of the aliphatic chain, which is also an electron donor, but weaker than the OH group.⁴⁹ Both groups have the ability to direct the entry of new substituents to the *ortho* positions into the aromatic ring. However, each of these groups causes different degrees of steric hindrance in the positions of the new groups in the ring, as demonstrated in Figure 5. Therefore, it is unlikely for the reaction to occur at carbon 2, due to the strong steric hindrance caused by the proximity of the OH group and the free rotation of the long aliphatic chain of cardanol. Furthermore, between the two remaining entry positions, the incorporation in carbon 6 is expected to prevail, resulting from both the steric hindrance undergone by carbon 4, due to the proximity of the alkyl group and by the greater activation character of the OH group.⁴⁹ Furthermore, the increase in the viscosity of the system during the synthesis would cause a reduction in the reactivity of the other entry positions after the incorporation of the first group, making it unlikely that more than one alkyl group would be incorporated into the same ring.

Therefore, only two arrangements could be produced during the synthesis of the materials: structures with 1,2,5-trisubstituted or 1,3,4-trisubstituted configuration in relation to the OH group of the phenol, as demonstrated in Figure 6.

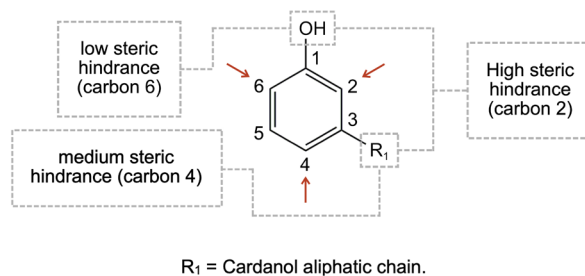


Figure 5. Indications of possible reaction positions of substituent groups on the aromatic ring of cardanol and steric hindrance relationship between cardanol substituent groups.

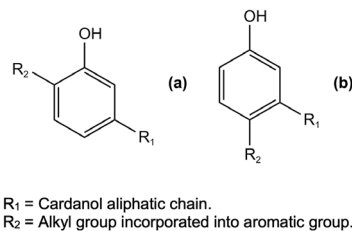


Figure 6. Possible structural arrangements of the aromatic ring in the synthesis products considering the configurations (a) 1,2,5-trisubstituted and (b) 1,3,4-trisubstituted in relation to the OH group of phenol.

To identify whether only one or both structural arrangements were produced during the synthesis, we used

formulas and correlation tables to estimate the chemical shifts of the aromatic hydrogens in each arrangement.⁵⁰ We calculated the predicted chemical shift of each proton by using equation 1, according to which the estimated shift of the proton (δ_{est}) is given by the sum of the base values of 7.27 and the summation of the adjustments of the chemical shifts ($\Sigma\delta_{\text{adj}}$) promoted by each substituent group present in the aromatic ring.

$$\delta_{\text{est}} / \text{ppm} = 7.27 + \Sigma\delta_{\text{adj}} \quad (1)$$

The chemical shift adjustment values for the two possible substituent groups in the structure of the aromatic ring of cardanol are reported in Table 2, including the values for the *ortho*, *meta* and *para* positions of the group in relation to the position of the proton evaluated.

Table 2. Adjustment values of the chemical shift of aromatic ¹H in relation to the possible substituent groups of the ring in the structure of the synthesized materials^a

Substituent group (-R)	Position group in relation to the evaluated ¹ H / ppm		
	δ_{ortho}	δ_{ortho}	δ_{ortho}
Alkyl	-0.14	-0.06	-0.17
OH	-0.53	-0.17	-0.45

^aAdapted from reference 50.

Figure 7 depicts the multiplicity of the expected signals and the estimated chemical shifts of the protons for the two predicted structural arrangements.

The calculations of the chemical shifts estimated for the protons H_a, H_b, and H_c in the 1,2,5-trisubstituted arrangement were equivalent to the chemical shifts and the multiplicity of signals observed in the spectra of the materials (Figure 4, d, δ 6.90, overlapping signs, δ 6.62 and s, δ 6.49), suggesting the occurrence of a structure

with the 1,2,5-trisubstituted arrangement in the synthesized products. On the other hand, in the estimated chemical shifts of the protons in the 1,3,4-trisubstituted arrangement, we noted that only the protons H_d and H_e had values and multiplicity allowing attributing them to the signals observed in the spectra. In this prediction, the proton H_f exhibited a multiplicity that did not coincide with the signal of δ 6.49 found in the spectra. Besides this, none of the protons contained in this arrangement had a chemical shift permitting attribution to the signal that appeared at δ 6.62 ppm in the spectra of the material. Unlike the previous arrangement, the calculated estimates and the signals forecast for the protons diverged from the pattern of the signals in the spectra, so we discarded the hypothesis of the existence of the 1,3,5-trisubstituted arrangement in the structure of the synthesized materials. The confirmation of the occurrence of the 1,2,5-trisubstituted arrangement indicated the existence of a favored position for incorporation of the substituent groups in the aromatic ring, as discussed previously.

It is also important to highlight that the spectra of the low-conversion materials (PACN2-1, PACN4-1, PDCN2-1, and PDCN2-2) showed a low-intensity signal at δ 4.13 ppm that was not observed for the other analyzed materials (PDCN2-3 and PDCN4-3). This signal is related to the occurrence of an etherification reaction involving the OH group of phenol.¹⁹ The low signal intensity suggests that this route was unfavorable during synthesis. In contrast, the absence of this signal in the spectra of the high-conversion products suggests that some factor would be responsible for inhibiting the etherification during the synthesis of these materials.

In the Friedel-Crafts aromatic alkylation mechanism, cardanol polymerization occurs mainly through the reaction between the carbocation and the aromatic ring.^{21,51} As

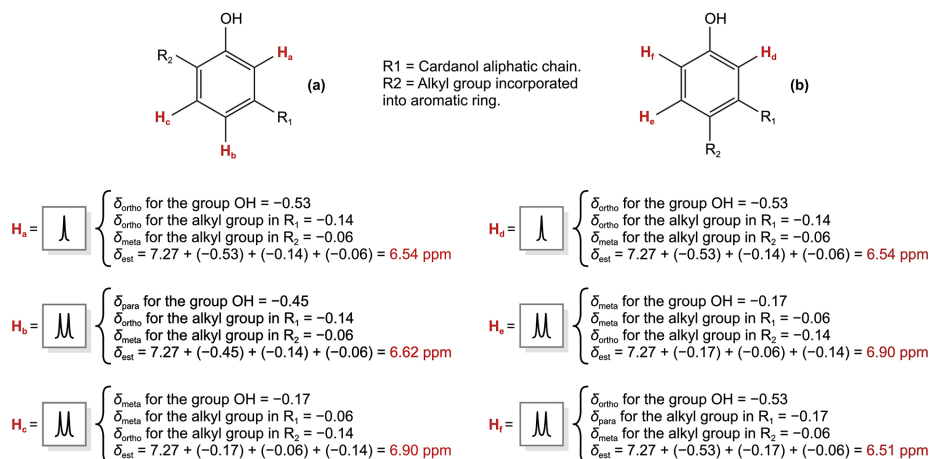


Figure 7. Expected signs and estimated chemical shifts estimates for aromatic ¹H in the structural arrangements: (a) 1,2,5-trisubstituted and (b) 1,3,4-trisubstituted.

chain propagation is interrupted soon after the formation of the active center (carbocation), the low concentration of initiator used to synthesize the materials PACN2-1, PACN4-1, PDCN2-1 and PDCN2-2 did not generate enough active centers to deplete the unsaturations of the compound. On the other hand, the attempt to use higher initiator concentrations (greater than 1%) using ACN led to the formation of crosslinked materials, which did not occur for the materials obtained from DCN. The explanation for this phenomenon lies in the ACN and DCN compositions differences, being possible to assume that the triolefinic structure is the factor responsible for the crosslinking of the material, where the reaction of the three unsaturations in the molecule promoted the joining of the polymer chains already formed in the reaction medium. In this case, the consumption of all the unsaturations in the triolefinic structure was directly related to the high availability of the initiator in the medium. Besides this, it enabled associating the triolefinic structure of cardanol with another phenomenon: the greater \bar{M}_n of the PACN2-1 and PACN4-1 in comparison with the other products. The presence of three unsaturations in the molecule increased the probability of the structure reacting again, thus enabling

the union of the two species already formed containing long chains, promoting the increment of these molar mass of the structures, leading to high \bar{M}_n of the material, as identified by the SEC analyses of the products obtained with ACN (Figure 1).

^{13}C NMR spectra of ACN and DCN

The ^{13}C NMR analyses corroborated many of the conclusions of the ^1H NMR analyses and elucidated other important aspects of the structure of the compounds studied. Figure 8 presents the interpretation of the ^{13}C NMR spectra of the reagents ACN and DCN, attributing the signals observed to the corresponding positions of each carbon nucleus in the structures of cardanol and cardol. For a better definition of the signals observed, we separated the spectra of the reagents and the synthesized materials into two regions. That division was possible because the region between 97.5 and 49.0 ppm in the spectra did not contain signals besides a triplet at 77.0 ppm, corresponding to CDCl_3 .

In the spectral region between 162.5 and 97.2 ppm, the signals at a (δ 155.5 ppm), b (δ 145.0 ppm),

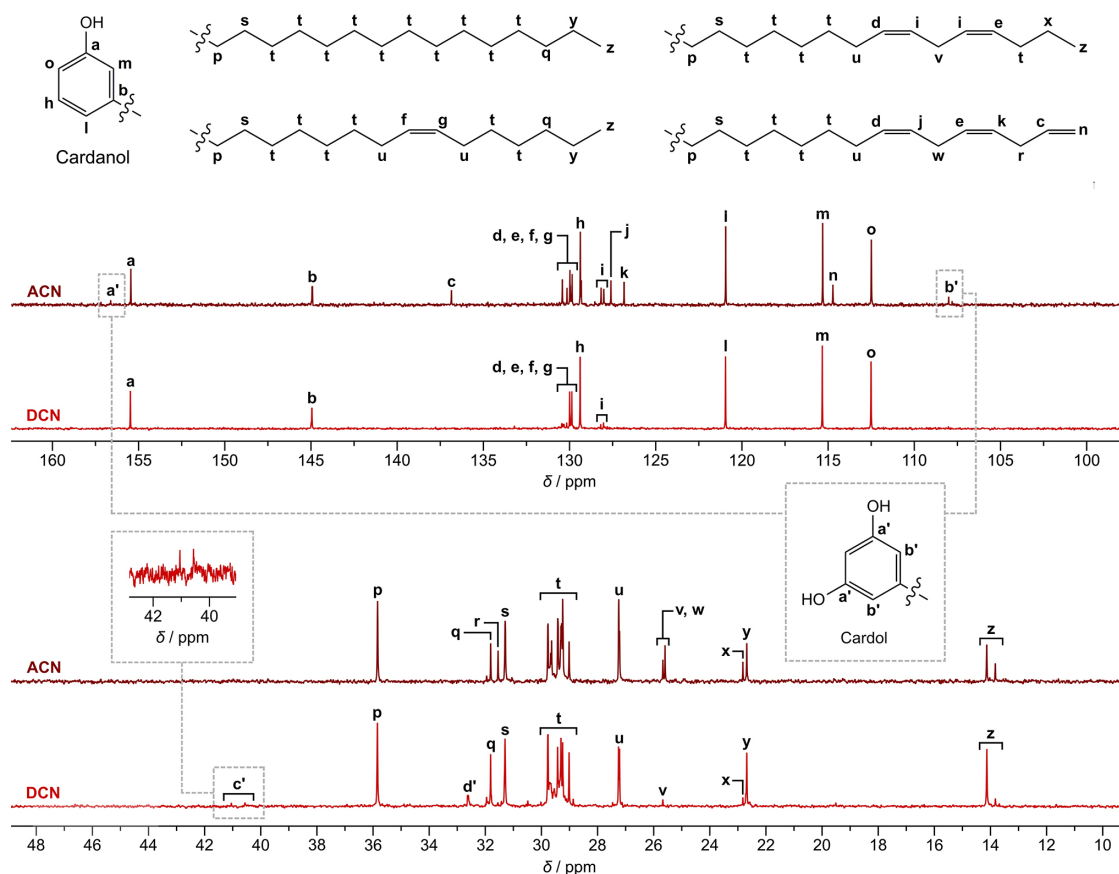


Figure 8. Comparison between the ^{13}C NMR spectra (125 MHz, CDCl_3) of ACN and DCN and signal assignment to each carbon in the four structures of cardanol and cardol.

h (δ 129.4 ppm), l (δ 120.9 ppm), m (δ 115.4 ppm) and o (δ 112.5 ppm) correspond to the carbon nuclei of the aromatic ring of cardanol and are present in both spectra.¹¹ The signals at c (δ 136.9 ppm) and n (δ 114.8 ppm) are related to the carbons of the vinyl group in the triolefinic structure.⁵² As already identified by the ¹H NMR analyses of the two reagents, this structure was not present in the spectra of the purified material, so these signals, as well as other signals related to this structure, are absent in the DCN spectrum. The signals at d (δ 130.5 ppm) and e (δ 130.2 ppm) refer to the unsaturation carbons present in the di and triolefinic structures.⁵³ In the DCN spectrum, these signals have lesser intensity than the same signals in the ACN spectrum, as a result of the absence of the triolefinic structure in the distilled material. The signals at f (δ 130.0 ppm) and g (δ 129.9 ppm) are attributed to the unsaturated carbons in the mono-olefinic structure and are present in the spectra of both reagents. Due to the increased concentration of this species in the composition of the distilled material, both signals are more intense in the DCN spectrum.

The two signals at i (δ 128.2 and 128.0 ppm), in turn, refer to the unsaturation carbons present only in the diolefinic structure. These signals are less intense in the DCN spectrum, confirming the hypothesis established during the analysis of the ¹H NMR spectrum of the material, that only a small fraction of this structure was distilled during the purification of the compound. In turn, the signals at j (δ 127.6 ppm) and k (δ 126.8 ppm) refer to the unsaturation carbons present in the triolefinic structure, and naturally were not observed in the DCN spectrum due to the absence of this structure in the composition of the purified material.

Furthermore, in this spectral region the signals at a' (δ 156.0 ppm) and b' (δ 108.0 ppm), were only found in the ACN spectrum, referring to the four carbon nuclei of the aromatic ring of cardol.⁵⁴ The total absence of signals referring to cardol in the DCN spectrum is related to the reduction of these species in the final composition of the distilled material.

In the second region of the spectrum, between 48.0 and 11.0 ppm, the signal at p (δ 35.9 ppm) corresponds to the carbon of the aliphatic chain linked directly to the aromatic ring in all four structures of cardanol, and thus occurs in both spectra. The signal at q (δ 31.8 ppm) is attributed to the methylene carbons (CH₂) located at two positions of the methyl carbon (CH₃) in the side chain of the saturated and mono-olefinic structures of cardanol, also present in both spectra. The signal at r (δ 31.6 ppm) is attributed to the carbon positioned between an unsaturation and the vinyl group in the triolefinic structure. This was one more signal referring to a carbon present only in this spectrum; it was not observed in the DCN spectrum. The signal at

s (δ 31.3 ppm) is attributed to the second carbon of the aliphatic chain near the aromatic ring in all the structures, occurring in both spectra. In turn, the group of signals at t (δ 30.0-29.0 ppm), observed in both spectra, refers to the CH₂ carbons in the side chains of all four structures. The two signals at u (δ 27.3 and 27.2 ppm) correspond to the carbons adjacent to the double bonds in the three unsaturated structures of cardanol. Due to the absence of the triolefinic structure in the purified material, the signal at δ 27.3 ppm had lesser intensity in the DCN spectrum than the signal in the ACN spectrum. The signals at v (δ 25.7 ppm) and w (δ 25.6 ppm) correspond to the carbon positioned between two unsaturations in the diolefinic and triolefinic structures, respectively. Because of the absence of the triolefinic structure in the purified material, the signal at w was absent in the DCN spectrum. The signal at x (δ 22.8 ppm) is also attributed only to the diolefinic structure, corresponding to the CH₂ carbon adjacent to the CH₃ carbon in the side chain of the structure. The lower intensity of this signal and the signal at v in the DCN spectrum in relation to the ACN spectrum provide further evidence that the diolefinic structure was not distilled totally in the purified material. The signal at y (δ 22.7 ppm) also refers to the carbon adjacent to the CH₃, this time in the saturated and mono-olefinic structures of cardanol. Finally, the two signals at z (δ 14.2 and 13.9 ppm) refer to the terminal CH₃ carbon of the aliphatic chain of cardanol. The signal at δ 14.2 ppm corresponds to the CH₃ carbon in the saturated and mono-olefinic structures and the signal at δ 13.9 ppm corresponds to the CH₃ of the diolefinic structure. This last signal was less intense in the DCN spectrum due to the smaller concentration of this structure in the composition of the purified material.

Besides the signals referring to structure of cardanol, in the spectrum of the DCN reagent we observed two signals with weak intensity at c' (δ 41.0 and 40.5 ppm). This region of the spectrum corresponds to the signals of the methine carbons (CH) and their occurrence in the DCN spectrum indicates the formation of this type of carbon in the structure of the distilled material. Since cardanol originally does not have CH carbons in its structure, the nuclei could have been produced by a chain reaction between the double bonds of the side chain of the cardanol molecule, so the presence of these signals in the DCN spectrum, even at low intensity, suggests the occurrence of polymerization reactions in the material. Due to the absence of the initiator BF₃·O(C₂H₅)₂, those reactions almost certainly involve radical initiation, triggered by the heating of the material during distillation. That assumption makes sense, since the ¹H NMR spectra of this reagent, unlike those of the synthesized products, did not have signals referring to the modification of the

structure of the aromatic ring of cardanol. Besides this, another signal, more intense, also was observed in the DCN spectrum at δ 32.6 ppm, which likely is associated with some structure resulting from the reactions that occurred during the heating of the material.

^{13}C NMR spectra of the synthesized materials

Figure 9 presents the first region of the ^{13}C NMR spectra of the six synthesized products, revealing significant differences between the observed signals. Some of them derive from variations in the conversion of the olefinic groups in the different synthesized products. The occurrence of the signals referring to these groups is in accordance with the observation described previously in the ^1H NMR analyses of the materials, i.e., the spectra of the PACN2-1, PACN4-1 and PDCN2-1 had signals referring to the olefinic groups of the three unsaturated structures of cardanol, while the spectrum of PDCN2-2 only had signals referring to mono-olefinic cardanol and the spectra of PDCN2-3 and PDCN4-3 did not have any signal.

Regarding the signals referring to the modification of the aromatic ring structure of cardanol, only in the spectra

of PDCN2-3 and PDCN4-3 are all signals present (δ 153.2, 141.4, 127.5 and 115.3 ppm) that can be attributed to the alteration of the ring. Two of these signals (δ 127.5 and 115.3 ppm) are also present in the spectrum of PDCN2-2, but with less intensity than the signals occurring in the spectra of the two high-conversion products. The partial or total absence of signals related to the modification of the ring in the spectra of the low-conversion materials can be attributed to the low abundance of nuclei able to generate resonance in the structure of the reaction products.⁵⁰

Finally, for the product PDCN2-3 we observed four signals (δ 137.8, 129.1, 128.3 and 125.4 ppm), related to the solvent toluene utilized to remove the material from the reaction flask after synthesis.

Figure 10 presents the second region of the ^{13}C NMR spectra of the six synthesized products, where differences between the spectra are observed. Besides the occurrence of new signals at δ 35.5 and 32.0 ppm, common to all the materials, the products with low conversion (PACN2-1, PACN4-1, PDCN2-1, and PDCN2-2) had signals of δ 36.1, 34.0, 32.6 and 25.4 ppm, along with a low-intensity signal at δ 27.7 ppm in the spectrum of the PDCN2-2. In counterpart, the spectra of the products with high conversion (PDCN2-3

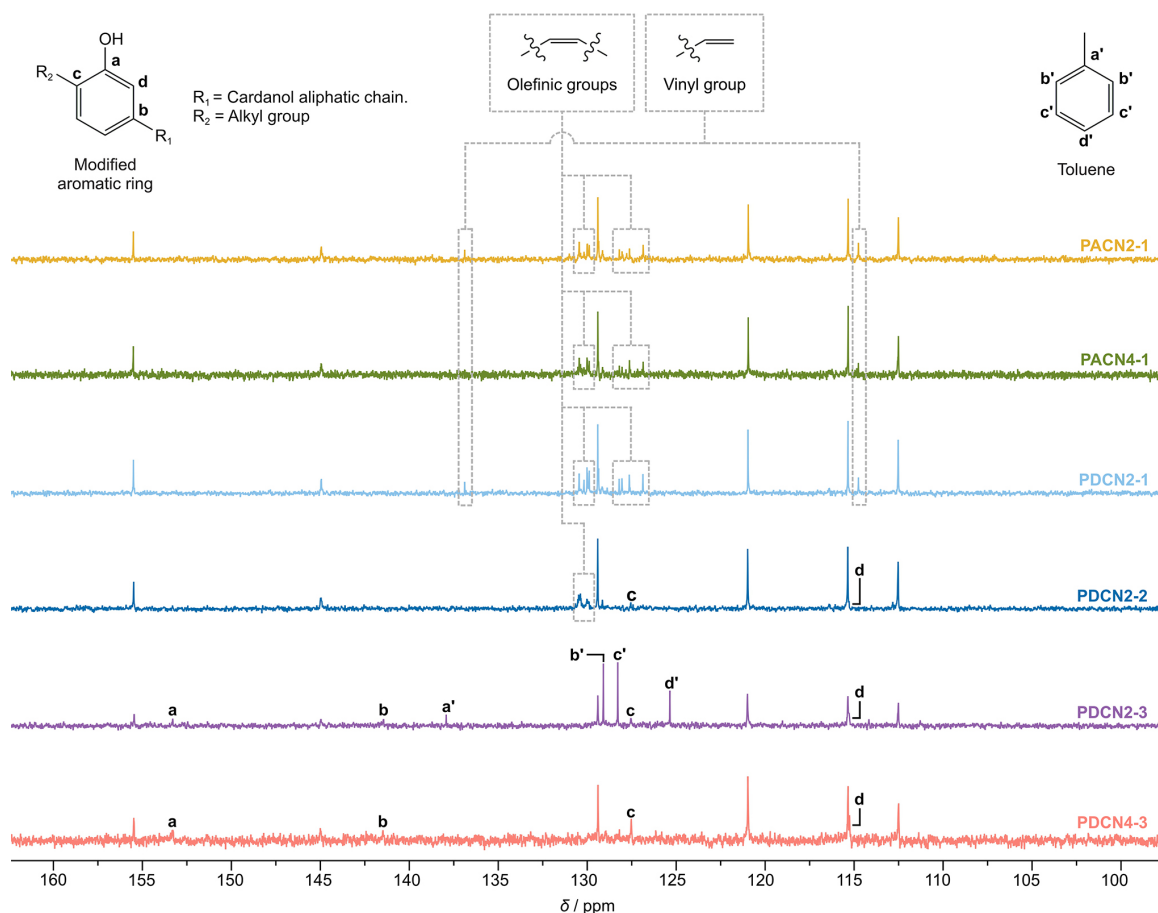


Figure 9. Comparison of ^{13}C NMR spectra (125 MHz, CDCl_3) of synthesized materials in the region between 162.5 and 97.5 ppm.

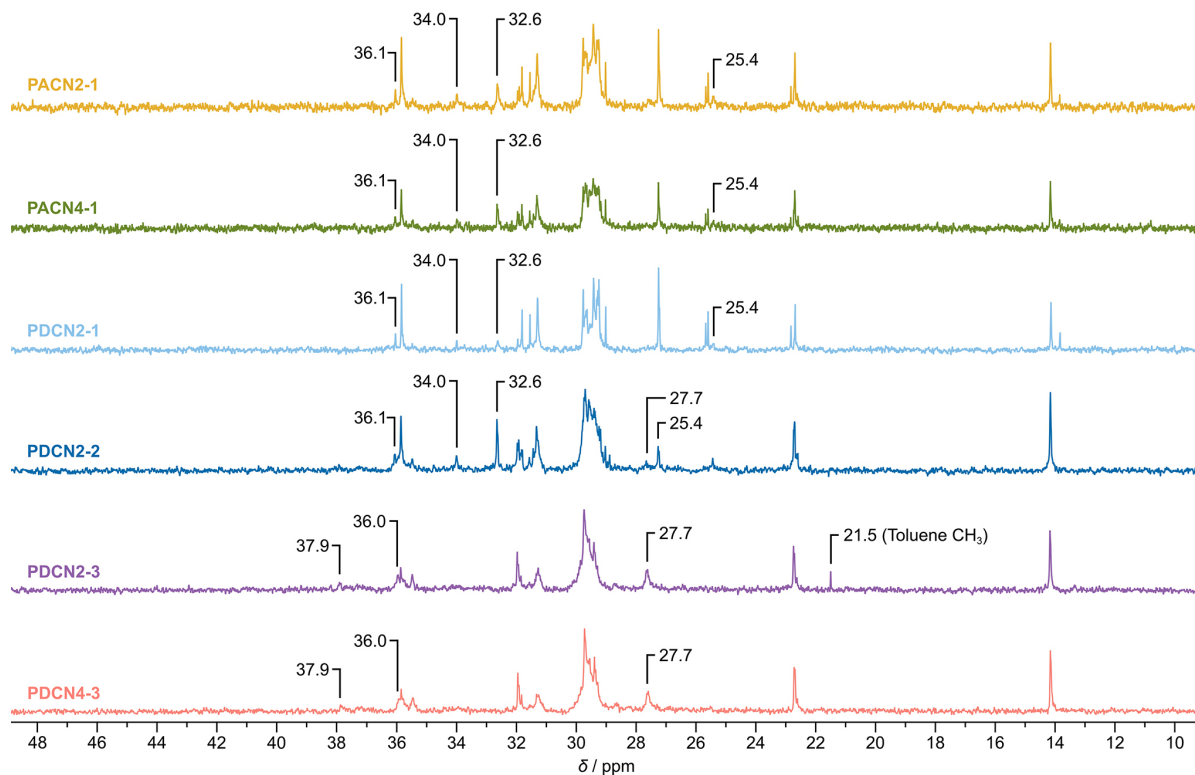


Figure 10. ^{13}C NMR spectra (125 MHz, CDCl_3) of synthesized materials in the region between 49.0 and 9.0 ppm.

and PDCN4-3) presented new signals at δ 37.9, 36.0, and 27.7 ppm. The divergences found in the spectra confirm the existence of structural differences in the synthesis products of these materials, as suggested by the occurrence of the signals at δ 1.89 and 4.13 ppm in the ^1H NMR spectra of the materials with low conversion (Figure 3).

The absence of signals in the region between 97.5 and 49.0 ppm, related to the protons of CH_2 in an ether bond, confirms low etherification during the synthesis of the PACN2-1, PACN4-1, PDCN2-1, and PDCN2-2. The low incidence of this reaction agrees with no crosslinking observation. In this case, the etherification reaction would be limited to the incorporation of branches in the polymer chain.

The structural differences among the reaction products must be related to the differences in the monomers compositions. ACN has cardanol in all its structures, including the triolefinic one. However, the crosslinking observed during the synthesis of this compound together with the fact the products obtained from it had a low conversion, makes the complete conversion of the triolefinic structure during the synthesis of the PACN2-1 and PACN4-1 unlikely. Another important characteristic, now related to the diolefinic structure, is the reduction of its concentration in the composition of DCN promoted by ACN purification.

Previously, the analyses of the ^1H NMR spectra allowed identifying the position of incorporation of the substituent

group in the aromatic ring but based on factors such as the structural variation of cardanol, differences in the composition of the reagents and the occurrence of the rearrangements identified earlier (Scheme 1), different structures could have been produced, depending on the position of the charge of the carbocation in the aliphatic chain, during the reaction with the ring, whether located at the opening position of a double bond or after the migration of the charge promoted by the rearrangements. Based on these observations, we can assume the formation of three main structures, generated from the diolefinic, monoolefinic and saturated structures of cardanol, as presented in Figure 11.

The triolefinic structure, abundant in ACN composition and identified in the product obtained by synthesizing PDCN2-1, was not considered for prediction of the structures formed, since in the case of maximum conversion of the unsaturations contained in this structure, the ^{13}C nuclei of the aliphatic chain, linked directly to the three aromatic rings, produced signals equivalent to the sum of the signals generated by structures **1** and **2**. Therefore, the signals generated by this product prevented distinguishing it from the other structures produced. The structure formed by the reaction of diolefinic cardanol with only one aromatic ring was also not considered in this prediction, since this structure possibly did not generate signals with sufficient intensity in the spectra, given the abundance of the structure

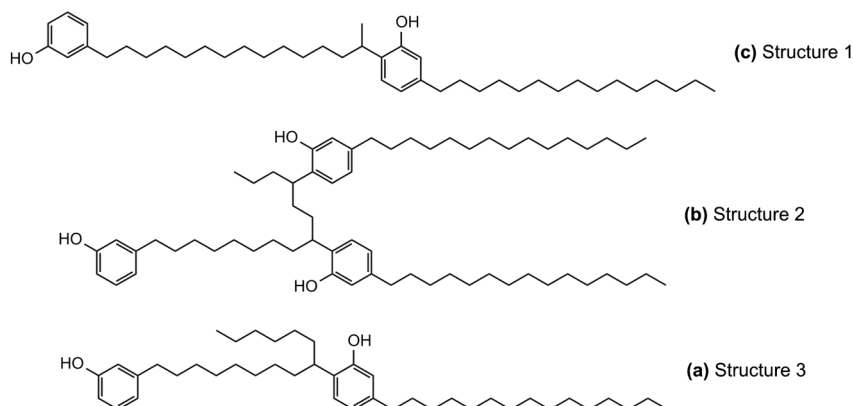


Figure 11. Possible structures generated after the reaction of the aromatic ring with the carbocation generated (a) in the position of charge migration after rearrangement, (b) in the two positions of the opening of the double bonds in the diolefinic cardanol and (c) in the opening position of the double bond in the mono-olefinic cardanol.

containing two unsaturations in the composition of the reagents, as previously mentioned.

In an attempt to identify if one of the proposed structures, or more than one of them, was present in the synthesis products, we performed calculations of the estimated chemical shifts for nuclei around the bond formed between the aliphatic chain and aromatic ring in the structures considered (Figure 11), using the ChemDraw® software.⁴¹ Figure 12 shows three proposed structures, highlighting in each one the carbon nuclei whose chemical shift was calculated, as well as the estimated value of each nucleus.

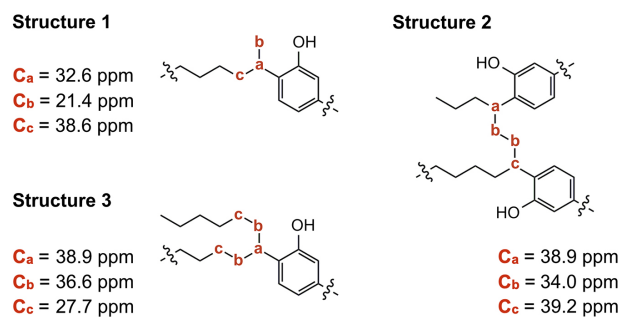


Figure 12. Estimated chemical shifts of carbons around the bond formed between the aromatic ring and the aliphatic chain in the three structures considered in Figure 11.

In structure **1**, only the nuclei C_a can be attributed to one of the signals observed in the spectra of the PACN2-1, PACN4-1, PDCN2-1 and PDCN2-2. This nucleus has a calculated shift identical to the signal of δ 32.6 ppm in the spectra of these materials. Since these spectra are associated with products having a low conversion of the reagent, the absence of signals that can be attributed to the nuclei C_b and C_c , could be related to the low abundance of resonant nuclei in the structures generated during the synthesis of the material.

Among the estimates carried out for the carbons in structure **2**, only the nucleus C_b exhibited a calculated shift,

which can be attributed to one of the signals observed in the spectra of PACN2-1, PACN4-1, PDCN2-1, and PDCN2-2, with this shift being identical to the signal of δ 34.0 ppm in the spectra. This nucleus corresponds to two carbon atoms in equivalent chemical environments in this structure, differing from the other calculated nuclei, which represent individual nuclei in the evaluated structure. Considering the concentration of the diolefinic structure in the composition of ACN (ca. 17%)⁴ and the fact that this species has a low concentration in the composition of DCN, the absence of the signals referring to the nuclei C_a and C_c in the spectra of the products with low conversion is certainly related to the fact these two nuclei are located in distinct chemical environments in comparison with the pair of nuclei C_b , thus contributing to the low abundance of nuclei able to generate resonance in this position in the structure of the product.

Finally, the three nuclei evaluated in structure **3** had corresponding signals in the spectra of the products PDCN2-3 and PDCN4-3. This structure has a single nucleus, C_a which can be attributed to the signal of δ 37.9 ppm in the spectra, and two pairs of nuclei C_b and C_c in equivalent chemical environments, which can be attributed in the spectra respectively to the signals of δ 36.0 and 27.7 ppm. The presence of the signal δ 27.7 ppm with low intensity in the spectrum of PCND2-2, despite the absence of the two other signals in the spectra of the materials with high conversion, is evidence of the presence, albeit small, of structure **3** in the product of synthesizing this material. Based on the consideration that this material had higher conversion than samples PACN2-1, PACN4-1, and PDCN2-1, it is possible to assume that this structure depends on the occurrence of high conversion of the reagent during synthesis.

To check the hypotheses established from analyzing the estimated chemical shifts of the nuclei in the three proposed structures, and seeking to contemplate the materials with high and low conversion, we performed DEPT-135 NMR

analysis of the two products that showed divergent signals in the spectra (samples PACN4-1 and PDCN4-3). Figure 13 contains these spectra, indicating the type of carbon to which the signals refer, related to nuclei in the proposed structures.

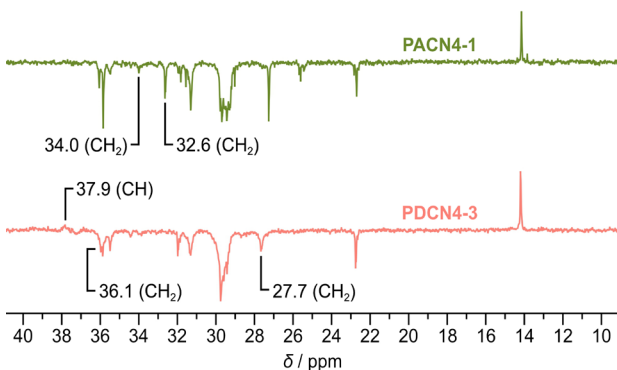


Figure 13. DEPT-135 NMR spectra (125 MHz, CDCl_3) of the materials PACN4-1 and PDCN4-3 in the region between 41.0 and 9.0 ppm.

In the spectrum of the product with low conversion (PACN4-1), the two signals (δ 32.6 and 34.0 ppm) that were related to proposed structures **1** and **2**, respectively, are in a negative phase, revealing that the signals observed refer to the CH_2 carbons in the structures of the synthesized product. The nucleus C_a calculated for structure **1** corresponds to a CH carbon (Figure 12), leading to the rejection of the hypothesis that the signal δ 32.6 ppm in the spectra of the materials with low conversion refers to this nucleus in the proposed structure. This result reveals that structure **1** (Figure 11) was not produced during the synthesis of the materials with low conversion. In contrast, the DEPT analysis enabled considering the formation of structure **2**, since the pair of nuclei C_b calculated for this structure, which were associated with the signal of δ 34.0 ppm, also refer to CH_2 carbons.

Contrary behavior was observed for the spectrum of PDCN4-3, where all the signals observed (δ 37.9, 36.6 and 27.7 ppm) had phases corresponding to the types of nuclei calculated for structure **3** (carbons CH, CH_2 , and CH_2 , respectively). This result corroborates the hypothesis of the formation of structure **3** (Figure 11) during the synthesis of the materials PDCN2-2, PDCN2-3 and PDCN4-3. The formation of this structure only in the products with high conversion is evidence that the occurrence of rearrangements is in fact related to the low conversion of the reagent during the synthesis of polycardanol.

Since all the signals generated in the PACN4-1 spectrum corresponded to CH_2 carbons, the signal at δ 32.6 ppm might have been related to a fourth type of product, where the structure formed did not contain CH nuclei. To produce that species, the rearrangement during the synthesis would have to promote the migration of the carbocation charge to the carbon 15' position at the end of the aliphatic chain of the monomer (instead of carbon 14', as considered previously in Scheme 1). Because this would be a primary carbocation, the charge would have to be stabilized by a negative ion present in the reaction medium, a function that could be performed by a molecule of diethyl ether released by the initiator $\text{BF}_3 \cdot \text{O}(\text{C}_2\text{H}_5)_2$ in the initial steps of the reaction. To confirm this new hypothesis, we carried out a 2D DEPT-HSQC analysis of the PACN4-1. Figure 14 depicts the spectrum obtained and correlates it with the signals evaluated between the spectra of carbon and hydrogen.

This analysis revealed that the signal at δ 32.6 ppm in the ^{13}C NMR spectrum was correlated with the signal at δ 1.51 ppm in the ^1H NMR spectrum. The signal at δ 1.51 ppm was already present in the spectra of the reagents (Figure 2), referring to the protons located in the

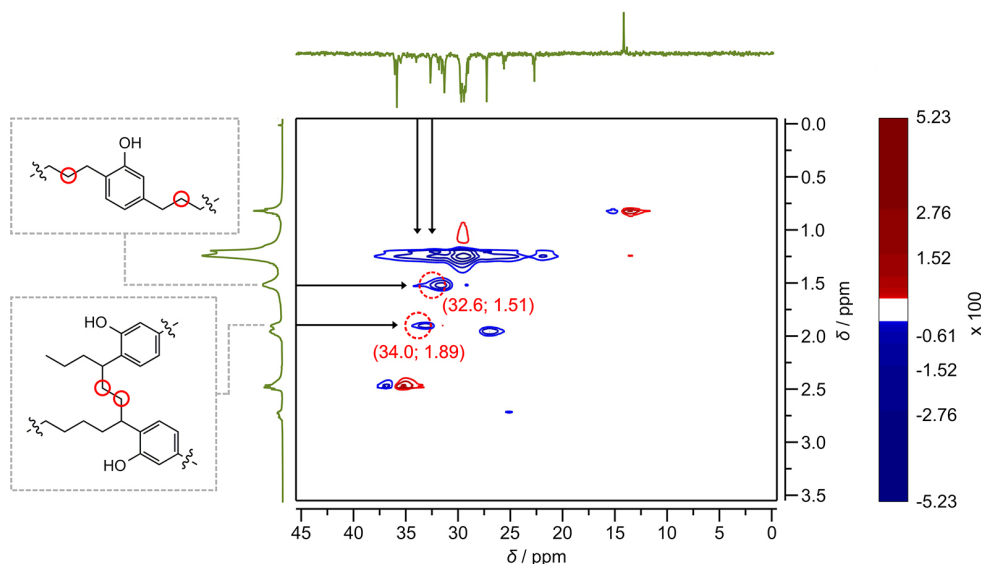


Figure 14. 2D DEPT-HSQC spectrum of the material PACN4-1.

second carbon of the aliphatic chain near the aromatic ring. In this case, the signal corresponded both to the original cardanol proton (correlated with the signal at δ 31.3 ppm in the ^{13}C NMR spectrum), and the proton of the aliphatic chain incorporated in the aromatic ring after the reaction, as demonstrated in Figure 14. This result can be considered an indication of the formation of this structure during the synthesis of the materials with low conversion. In turn, the signal at δ 34.0 ppm in the ^{13}C NMR spectrum is correlated with the signal at δ 1.89 ppm in the ^1H NMR spectrum, which arose in the spectra of the low-conversion materials (Figure 3). This signal appears in the lower field of the spectrum due to the deshielding effect caused by the proximity of the nuclei to the two aromatic rings.

Based on the results obtained, we can correlate the production of the different structures during the synthesis of the materials with the conversion rate of the reagent during the synthesis. The presence of different structures in the low-conversion products (PACN2-1, PACN4-1, PDCN2-1 and PDCN2-2) can be attributed to the low viscosity of the reaction system during the process of forming the polymer. The low initiator concentration, and consequently the smaller quantity of active centers generated during the synthesis, apparently moderately increased the viscosity of the medium, yielding cardanol molecules with greater mobility, along with sufficient time to promote the necessary rearrangements suggested in Scheme 1.

The opposite effect would explain the formation of structure **3** (Figure 11) only in the products PDCN2-3 and PDCN4-3, due to the high conversion of the reagent, promoted by the higher initiator concentrations used. The increased viscosity of the reaction medium in the initial steps of the reaction would diminish the mobility of the structures during the synthesis. As a consequence, there would be insufficient time for rearrangement of the carbocation in the aliphatic chain of cardanol, thus inhibiting the formation of other structures in these synthesis products. The absence of structure **2** (Figure 11) in these materials also is probably related to the increased viscosity of the reaction medium, where the incorporation of an aromatic ring in the diolefinic structure hampers the incorporation of a second ring in

the same structure, even after the opening of the second unsaturation. In this case, the charge of the carbocation could remain living in the structure of the molecule, or in a more specific case, could be transferred to a nearby secondary aliphatic chain. This does not mean that the presence of two aromatic rings in a single aliphatic chain of cardanol in high-conversion materials is improbable. However, due to the reaction conditions involved in the synthesis of these materials, such occurrence could be reduced, also contributing to the absence of the signals in the spectra, due to the low abundance of resonant nuclei in the structure of the material produced. Based on these observations, we can conclude that just as in the case of an increase in molar mass, the majority product of the reaction of cardanol is intrinsically dependent on the initiator concentration. In addition, the lower mobility presented by the intermediate structures during the synthesis of high-conversion products should also contribute to inhibiting the etherification reactions, as observed in the ^1H NMR spectra of these materials (Figure 3).

The products generated in the low conversion reactions are highly complex, mainly due to the possibility of species containing unsaturations being incorporated into the structure of macromolecules, besides the possibility of rearrangements and occurrence of etherification reactions in the structure of the phenol group, preventing the identification of all species formed during the synthesis. In contrast, the structural characterization of the high-conversion materials left no doubts about the main product formed, allowing its precise description. Figure 15 shows the general structure of the high-conversion polycardanol, considering the contributions of the structures present in the DCN. It is possible to suppose that the structure of the material can even exhibit branches due to the contribution of the diolefinic cardanol, although to a small extent because of the low concentration of this species in the reagent.

Conclusions

Depending on the reaction conditions, the synthesis of polycardanol from cardanol and $\text{BF}_3 \cdot \text{O}(\text{C}_2\text{H}_5)_2$ produces

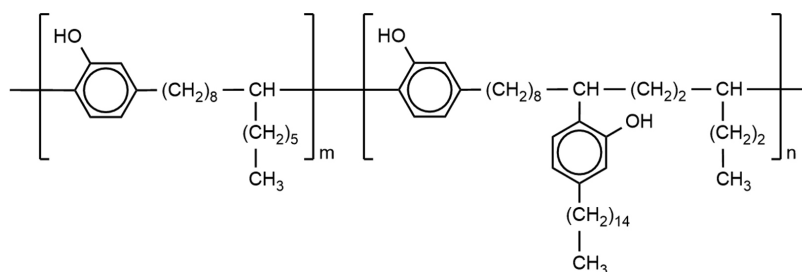


Figure 15. Generic structure of polycardanol for products that exhibited maximum conversion, considering the contributions of mono and diolefinic structures of cardanol.

materials with different molar masses, dispersities, and molecular structures, besides distinguish conversions, which were elucidated by this work.

Although the synthesis of the material occurs mainly through a Friedel-Crafts aromatic alkylation mechanism, other parallel reactions take place such as rearrangements from migrations of hydride ions and etherification of the phenol group. The rearrangement of the carbocation charge is responsible for the formation of a vinyl group in the different cardanol structures, generating a triolefinic structure, that was not present in the distilled cardanol. By intra or intermolecular rearrangements it is possible to form a primary carbocation during the synthesis of low-conversion materials. In turn, the etherification reaction, which could be responsible for the crosslinking reaction, is inhibited in the systems presenting high viscosity, and occurs in a low extension in the low-conversion reactions, generating branches in the polymer chains.

For distilled cardanol, the conversion rate is increased as increasing initiator concentration in the range tested (1-3% m/m). The main products of the high conversions are structures containing the aromatic ring directly linked where the charge of the carbocation is generated in the aliphatic chain of the monomer, and structures most similar to each other are formed. In contrast, the low-conversion materials, due to the low viscosity of the medium, produce a wide variety of structures that are difficult to identify. The molar mass of the polymer also increases as increasing initiator concentration.

The presence of triolefinic structure in the aged cardanol was responsible for two important phenomena involving the synthesis mechanism: the crosslinking of the material when using relatively high concentrations of the initiator, and the increase in molar mass dispersity.

Supplementary Information

Supplementary data are available free of charge at <http://jbcs.sbc.org.br> as PDF file.

Acknowledgments

The authors would like to thank CAPES (financial code 001), CNPq (303583/2019-3) and FAPERJ (E-26/200.974/2021) for their financial support and the Polymerization Engineering Laboratory (EngePol/Coppe/UFRJ) and the Liquid Nuclear Magnetic Resonance Laboratory (LABRMN-2/IQ/UFRJ), by size exclusion chromatography and nuclear magnetic resonance analyses, respectively.

References

1. Chen, J.; Nie, X.; Liu, Z.; Mi, Z.; Zhou, Y.; *ACS Sustainable Chem. Eng.* **2015**, *3*, 1164. [Crossref]
2. Wang, H.; Zhou, Q.; *ACS Sustainable Chem. Eng.* **2018**, *6*, 12088. [Crossref]
3. Walters, C. M.; Matharu G. K.; Hamad, W. Y.; Lizundia, E.; MacLachlan, M. J.; *Chem. Mater.* **2021**, *33*, 5197. [Crossref]
4. Balgude, D.; Sabnes, A.; Ghosh, S. K.; *Eur. Polym. J.* **2016**, *85*, 620. [Crossref]
5. Can, E.; Kınacı, E.; Palmese, G. R.; *Eur. Polym. J.* **2015**, *72*, 129. [Crossref]
6. Sung, J.; Sun, X. S.; *Prog. Org. Coat.* **2018**, *123*, 242. [Crossref]
7. Cardoso, J. J. F.; Ricci-Júnior, E.; Gentili, D.; Spinelli, L. S.; Lucas, E. F.; *Quim. Nova* **2018**, *41*, 273. [Crossref]
8. Bachalaran, V. S.; Jadhav, S. R.; Vemula, P. K.; John, G.; *Chem. Soc. Rev.* **2013**, *42*, 427. [Crossref]
9. Patel, R. N.; Bandyopadhyay, S.; Ganesh, A.; *Bioresour. Technol.* **2006**, *97*, 847. [Crossref]
10. Mazzetto, S. E.; Lomonaco, D.; Mele, G.; *Quim. Nova* **2009**, *32*, 732. [Crossref]
11. Costa, K. P.; de Viveiros, B. M.; Schmidt Jr., M. A. S.; Suarez, P. A. Z.; Rezende, M. J. C.; *Fuel* **2019**, *235*, 1010. [Crossref]
12. Voirin, C.; Caillol, S.; Sadavarte, N. V.; Tawade, B. V.; Boutevin, B.; Wadgaonkar, P. P.; *Polym. Chem.* **2014**, *5*, 3142. [Crossref]
13. Ganfoud, R.; Guigo, N.; Puchot, L.; Verge, P.; Sbirrazzuoli, N.; *Eur. Polym. J.* **2019**, *119*, 120. [Crossref]
14. Vasapollo, G.; Mele, G.; Del Sole, R.; *Molecules* **2011**, *16*, 6871. [Crossref]
15. Wang, H.; Zhang, C.; Zeng, W.; Zhou, Q.; *Prog. Org. Coat.* **2019**, *135*, 281. [Crossref]
16. Biswas, A.; Alves, C. R.; Trevisan, M. T. S.; Berfield, J.; Furtado, R. F.; Liu, Z.; Cheng, H. N.; *J. Braz. Chem. Soc.* **2016**, *27*, 1078. [Crossref]
17. Manda, B. R.; Prasad, A. N.; Thatikonda, N. R.; Lacerda Jr., V.; Barbosa, L. R.; Santos, H.; Romão, W.; Pavan, F. R.; Ribeiro, C. M.; dos Santos, E. A.; Marques, M. R.; de Lima, D. P.; Micheletti, A. C.; Beatriz, A.; *J. Braz. Chem. Soc.* **2018**, *29*, 639. [Crossref]
18. Byun, H. Y.; Choi, M. H.; Chung, I. J.; *Chem. Mater.* **2001**, *13*, 4221. [Crossref]
19. Shishlov, O. F.; Dozhdikov, S. A.; Glukhikh, V. V.; Stoyanov, O. V.; *Polym. Sci., Ser. D* **2014**, *7*, 61. [Crossref]
20. Chen, Y.-P.; He, X.-Y.; Dayo, A. Q.; Wang, J.-Y.; Liu, W.-b.; Wang, J.; Tang, T.; *Polymer* **2019**, *179*, 121620. [Crossref]
21. Bai, W.; Xiao, X.; Chen, Q.; Xu, Y.; Zheng, S.; Lin, J.; *Prog. Org. Coat.* **2012**, *75*, 184. [Crossref]
22. Rocha Jr., L. C.; Ferreira, M. S.; Ramos, A. C. S.; *J. Pet. Sci. Eng.* **2006**, *51*, 26. [Crossref]
23. Laux, H.; Rahimian, I.; Butz, T.; *Fuel Process. Technol.* **2000**, *67*, 79. [Crossref]

24. Kraiwattanawong, K.; Folger, H. S.; Gharfeh, S. G.; Singh, P.; Thomason, W. H.; Chavadej, S.; *Energy Fuels* **2009**, *23*, 1575. [Crossref]
25. Mansur, C. R. E.; de Melo, A. R.; Lucas, E. F.; *Energy Fuels* **2012**, *26*, 4988. [Crossref]
26. Balestrin, L. B. S.; Frnacisco, R. D.; Bertran, C. A.; Cardoso, M. B.; Loh, W.; *Energy Fuels* **2019**, *33*, 4748. [Crossref]
27. Moreira, L. F. B.; González, G.; Lucas, E. F.; *Polímeros* **1998**, *8*, 46. [Crossref]
28. Afra, S.; Nasr-El-Din, H. A.; Socci, D.; Cui, Z.; *Fuel* **2018**, *220*, 481. [Crossref]
29. Alhreez, M.; Wen, D.; *Fuel* **2018**, *234*, 538. [Crossref]
30. Mazzeo, C. P. P.; Stedille, F. A.; Mansur, C. R. E.; Ramos, A. C. S.; Lucas, E. F.; *Energy Fuels* **2018**, *31*, 1087. [Crossref]
31. Honse, S. O.; Mansur, C. R. E.; Lucas, E. F.; *J. Braz. Chem. Soc.* **2012**, *23*, 2204. [Crossref]
32. Nunes, R. C. P.; Valle, M. R. T.; Reis, W. R. D.; Aversa, T. M.; Filipakis, S. D.; Lucas, E. F.; *J. Braz. Chem. Soc.* **2019**, *30*, 1241. [Crossref]
33. Zorzenão, P. C. S.; Mariath, R. M.; Pinto, F. E.; Tose, L. V.; Romão, W.; Santos, A. F.; Scheer, A. P.; Simon, S.; Sjöblom, J.; Yamamoto, C. I.; *J. Pet. Sci. Eng.* **2018**, *160*, 1. [Crossref]
34. Alimohammadi, S.; Zendeboudi, S.; James, L.; *Fuel* **2019**, *252*, 753. [Crossref]
35. Pereira, J. C.; López, I.; Salas, R.; Silva, F.; Fernández, C.; Urbina, C.; Lopez, J. C.; *Energy Fuels* **2007**, *21*, 1317. [Crossref]
36. Zendeboudi, S.; Shafiei, A.; Bahadori, A.; James L. A.; Elkamel, A.; Lohi, A.; *Chem. Eng. Res. Des.* **2014**, *92*, 857. [Crossref]
37. Firoozinia, H.; Abad, K. F. H.; Varamesh, A.; *Pet. Sci.* **2016**, *13*, 280. [Crossref]
38. Balestrin, L. B. S.; Loh, W.; *J. Braz. Chem. Soc.* **2020**, *31*, 230. [Crossref]
39. Moreira, L. F. B.; Lucas, E. F.; González, G.; *J. Appl. Pol. Sci.* **1999**, *73*, 29. [Crossref]
40. Ferreira, S. R.; Louzada, H. F.; Dip, R. M. M.; Gonzalez, G.; Lucas, E. F.; *Energy Fuels* **2015**, *29*, 7213. [Crossref]
41. ChemDraw® Professional, v.18.2.0.48; PerkinElmer Informatics, Inc., United States, 2018.
42. Loureiro, T.; Dip, R. M. M.; Lucas, E. F.; Spinelli, L. S.; *J. Polym. Environ.* **2017**, *26*, 555. [Crossref]
43. Rodrigues, F. H. A.; Souza, J. R. R.; França, F. C. F.; Ricardo, N. M. P. S.; Feitosa, J. P. A.; *e-Polym.* **2006**, *81*, 1. [Crossref]
44. Li, W. S. J.; Cuminet, F.; Ladmiraal, V.; Lacroix-Desmazes, P.; Caillol, S.; Negrell, C.; *Prog. Org. Coat.* **2021**, *153*, 106093. [Crossref]
45. Ladmiraal, V.; Jeannin, R.; Lizarazu, K. F.; Lai-Kee-Him, J.; Bron, P.; Laacroix-Desmazes, P.; Caillol, S.; *Eur. Polym. J.* **2017**, *93*, 785. [Crossref]
46. Fu, C.; Liu, J.; Xia, H.; Shen, L.; *Prog. Org. Coat.* **2015**, *83*, 19. [Crossref]
47. Silverstein, R. M.; Webster, F. X.; Kiemle, D. J.; *Spectrometric Identification of Organic Compounds*, vol. 1, 7th ed.; John Wiley & Sons: Danvers, United States, 2005.
48. Carey, F. A.; Sundberg, R. J.; *Advanced Organic Chemistry Part A: Structure and Mechanisms*, vol. 1, 5th ed.; Springer: New York, United States, 2007.
49. Solomons, T. W. G.; Frihle, C. B.; Snyder, S. A.; *Organic Chemistry*, vol. 2, 12th ed.; John Wiley & Sons: Hoboken, United States, 2016.
50. Pavia, D. L.; Lampman, G. M.; Kriz, G. S.; Vyvyan, J. R.; *Introduction to Spectroscopy*, vol. 1, 6th ed.; Cengage Learning: Stamford, United States, 2015.
51. Burstall, M. L. In *The Chemistry of Cationic Polymerization*; 1st ed.; Plesh, P. H., ed.; Pergamon Press: Germany, 1963.
52. da Silva, L. R. R.; Avelino, F.; Diogenes, O. B. F.; Sales, V. O. F.; da Silva, K. T.; Araujo, W. S.; Mazzetto, S. E.; Lomonaco, D.; *Prog. Org. Coat.* **2020**, *139*, 105449. [Crossref]
53. Jia, P.; Zheng, M.; Ma, Y.; Feng, G.; Xia, H.; Hu, L.; Zhang, M.; Zhou, Y.; *J. Clean. Prod.* **2019**, *206*, 838. [Crossref]
54. Maia, F. J. N.; Ribeiro, F. W. P.; Rangel, J. H. G.; Lomonaco, D.; Luna, F. M. T.; de Lima-Neto, P.; Correia, A. N.; Mazzetto, S. E.; *Ind. Crops Prod.* **2015**, *67*, 281. [Crossref]

Submitted: October 19, 2022

Published online: December 12, 2022

